Journal of Enzyme Inhibition and Medicinal Chemistry, February 2007; 22(1): 43–49

Isolation and characterization of N98-1272 A, B and C, selective acetylcholinesterase inhibitors from metabolites of an actinomycete strain

ZHI-HUI ZHENG[1,2], YUE-SHENG DONG[2], HUA ZHANG[2], XIN-HUA LU[2], XIAO REN[2], GUIYU ZHAO[1], JIAN-GONG HE[2], & SHU-YI SI[1]

[1]*Insitute of Medicinal Biotechnology, Chinese Academy of Medical Sciences, and Peking Union Medical College, Beijing 100050, China, and* [2]*New Drug Research & Development Center of North China Pharmaceutical Group Corporation, National Microbial Medicine Engineering & Research Center, Shijiazhuang 050015, China*

(Received 3 May 2006; accepted 30 July 2006)

Abstract

A high throughput screening was carried out in order to search for inhibitors of acetylcholinesterase (AChE) from microorganism metabolites. An actinomycete strain was found to produce active compounds named N98-1272 A, B and C with IC_{50} of 15.0, 11.5, 12.5 μM, respectively. Structural studies revealed that the three compounds are identical to the known antibiotics, Manumycin C, B and A. Kinetic analyses showed that N98-1272 C (Manumycin A) acted as a reversible noncompetitive inhibitor of acetylcholinesterase, with a Ki value of 7.2 μM. The cyclohexenone epoxide part of the structure plays a crucial role in the inhibitory activity against AChE. Compared with Tacrine, N98-1272 A, B, and C exhibit much better selectivity toward AChE over BuChE.

Keywords: *Alzheimer's disease, acetylcholinesterase, noncompetitive inhibitor, manumycin*

Introduction

Alzheimer's disease (AD) is a degenerative disorder of the central nervous system characterized clinically by the loss of memory, intellect and cognitive functions [1,2]. One of the explanations of etiology and pathophysiology of AD is that the cholinergic functions decline in the basal forebrain and cortex [3]. Accordingly, improvement of cholinergic function is regarded as a potential therapeutic approach to control Alzheimer's disease. Acetylcholine (ACh) is a major neurotransmitter. Acetylcholinesterase (AChE) catalyzes the hydrolysis of ACh within cholinergic synapses of the brain and autonomic nervous system which terminates the activity of ACh. One treatment strategy to enhance cholinergic functions is the use of AChE inhibitors to increase the availability of acetylcholine by blocking its degradation. AChE inhibitors are the only class of drugs currently approved in the United States for the treatment of AD. There are four AChE inhibitors currently available in the United States: Tacrine (Cognex®, 1993), donepezil (Aricept®, 1996), rivastigmine (Exelon®, 2000), and galantamine (Reminyl®, 2001) [4]. It has been shown that AChE inhibitor therapy significantly improves the cognitive and global functions in patients with Alzheimer's disease. In the course of our screening for AChE inhibitors, metabolites of an actinomycete strain N98-1272 were found to be inhibitors of AChE. Here we report the details of the fermentation and isolation of N98-1272. Moreover, the structure-activity relationship and inhibitory effect of compounds N98-1272 A, B and C on AChE are described.

Correspondence: S.Y. Si, Insitute of Medicinal Biotechnology, Chinese Academy of Medical Sciences and Peking Union Medical College, Beijing 100050, China. Tel: 86-10-63180604. Fax 86-10-63017302. E-mail: sisyimb@hotmail.com

ISSN 1475-6366 print/ISSN 1475-6374 online
DOI: 10.1080/14756360600988781

Materials and methods

Reagents

Recombinant human acetylcholinesterase (rhAChE E.C.3.1.1.7, one unit hydrolyzes 1.0 μmol of acetylcholine to choline and acetate per min at pH 8.0, 37°C), human butyrylcholinesterase (BuChE E.C.3.1.1.8, one unit hydrolyzes 1.0 μmol of butyrylthiocholine to choline and acetate per min at pH 8.0, 37°C), acetythiocholine (ATCh), butyrylthiocholine (BuTCh), dithiobisnitrobenzoate (DTNB) and Tacrine were all purchased from Sigma. All other chemicals were of analytical grade and purchased from commercial chemical companies including Sigma.

Microorganism

The producing strain, *actinomycete* N98-1272, was isolated from a soil sample collected from Xishuangbanna, Yunnan Province, People's Republic of China. It is a novel species of the genus *Streptomyces,* named *Streptomyces bannaensis* sp.nov. The bacteriological properties and taxonomic studies of strain *Streptomyces bannaensis* sp.nov have been previously described [5]. The strain was deposited in the China General Microbiological Culture Collection and the accession number is CGMCC No. 0762.

Analysis of Acetylcholinesterase and Butyrylcholinesterase activity

The inhibitory effects on AChE and BuChE were determined according to the method described by Ellman [6] with modification as follows: 0.08 unit of AChE or BuChE was dissolved in 50 μM potassium phosphate buffer (pH 7.4) and 2 μL of microorganism metabolite or purified compounds dissolved in DMSO were added to each well of a 96- well plate. After incubation with rhAChE (or rhBuChE) for 15 min at room temperature, 150 μL of ATCh (or BuTCh) and DTNB dissolved in 50 μM potassium phosphate buffer (pH 7.4) were added to a final concentration of 30 μM to each well. After incubation at 37°C for 1 h, the enzyme activity was analyzed by measuring the optical density (OD) at 405 nm (5-thio-2-nitrobenzoate) with a microplate reader (Wallac 1420 Victor2, PerkinElmer).

Initial studies on structure-activity relationship of N98-1272 C

To understand the structural constituents necessary for the activity of N98-1272 C, reduction of N98-1272 C was performed as described by Zeeck [7]. Briefly, 6.1 mg sodium borohydride was added to a stirred solution of 22 mg N98-1272 C in 5 mL dried MeOH. After 15 min, the solution was dissolved in 15 mL water, adjusted to pH 3.0 with 1.5 M oxalic acid and extracted with $CHCl_3$. The organic layer was dried, evaporated and chromatographically purified by HPLC (75%MeOH ~ 0.1% phosphoric acid) to obtain the yellow deoxy N98-1272 C. Its structure was confirmed by UV and MS spectra.

Inhibitory kinetics

In order to understand how N98-1272 C inhibits AChE, the initial rate of the enzyme was analyzed by measuring the formation of 5-thio-2-nitrobenzoate (yellow anion) at 405 nm wavelength UV. The reaction was carried out at 37°C for 5 min after pre-incubating AChE with various concentrations of N98-1272 C for 15 min. A plot of v (μmol /min/mL) versus [E] was obtained with different N98-1272C concentrations of 0 μM, 10 μM, 20 μM and different AChE concentrations of 0.01 ~ 0.16 U/well to distinguish between reversible or irreversible inhibition. A Hanes plot of [S]/v versus [S] was performed at ATCh concentrations in a range of 0.2–3.2 μM, with N98-1272 C concentrations of 0 μM, 10 μM, 20 μM.

Computational docking methods

The computational docking was carried out with FlexX run in SYBYL (version 7.1, Tripos Inc.). PDB file of co-crystal of an inhibitor [(RS)-(±)-Tacrine(10)-hupyridone] in the active site of acetylcholinesterase(PDB code 1ZGB) was used. Inhibitor (RS)-(±)-Tacrine hupyridone was extracted and used as a reference structure, that is, a fixed conformation docked into the active site of the enzyme. The docking conformations of the inhibitor Manumycin A were created with the FlexX and 30 docking conformations of Manumycin A were optioned. Each conformation was energy minimized with a molecular mechanics program. The high scoring conformation with a least RMS (root mean square) value compared with the reference structure was displayed to explain the interaction of Manumycin A and TcAChE. In the test of Manumycin A docking into the crystal structure of BuChE, the PDB file of co-crystal of hBuChE with butyrate (PDB code 1POI) was used.

Results

Fermentation

A loop of cells of *Streptomyces bannaensis* sp.nov from a solid slant was inoculated into 20 mL of seed medium composed of 5% glucose, 0.4% yeast extract, 0.4% Bacoto-tryptone (Difco), 0.4% beef extract, 0.2% NaCl, and 0.5% $CaCO_3$. The inoculated tubes were incubated on a reciprocating shaker at 28°C for 3 days. 5 mL of the seed culture was added to a 750 mL Erlenmeyer flask containing 120 mL medium consisting of 1% glucose, 1% soluble starch, 0.4% yeast

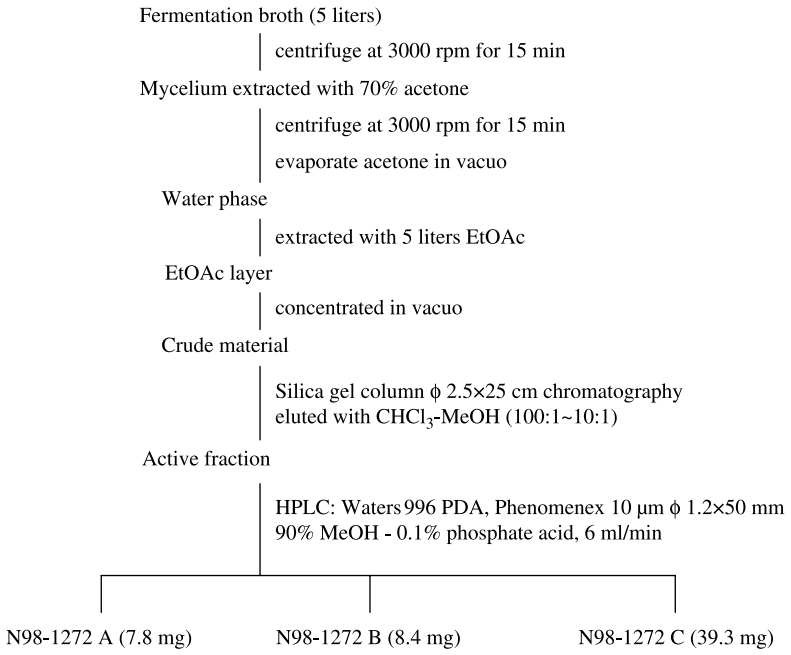

Figure 1. Isolation procedure for N98-1272 A, B, C.

extract, 0.4% Bacoto-tryptone (Difco), 0.4% beef extract, 0.2% NaCl, and 0.5% $CaCO_3$ and then incubated for 6 days on a rotary shaker (200 rpm) at 28°C. 5 liters of red mycelia broth was obtained from 50 flasks.

Isolation of N98-1272A, B and *C*

The isolation procedure for the active compounds is shown in Figure 1. Briefly, the broth of *Streptomyces bannaensis* sp.nov was centrifuged, and the mycelium was extracted with 75% acetone. After the insoluble mycelium remains were removed by centrifugation, the acetone was evaporated under reduced pressure. The concentrated aqueous solution was then extracted with ethyl acetate and the extract applied to a column of silica gel. The column was eluted with a gradient of chloroform-methanol from 100:1 to 10:1, and the active fractions were concentrated to dryness. Further purification was carried out by HPLC (Detector: Waters 996 PDA, Column: Phenomenex C18, 10 μm ϕ 1.2 × 50 mm) with mobile phase (solution of 90% MeOH-water with 0.1% phosphoric acid) and a flow rate of 6.0 mL/min at room temperature. Three active pure compounds, N98-1272 A (7.8 mg), N98-1272 B (8.4 mg) and N98-1272 C (39.3 mg) were obtained as yellow powders. UV, MS and NMR spectra studies indicated that the three compounds were identical to Manumycin B, C, A [7,8], and their structures are shown in Figure 2.

N98-1272 A (Manumycin B): Orange powder; UV (MeOH) λmax: 325.5 nm; ^{1}H NMR (500 MHz, DMSO-d_6): δ 7.29 (H-3), 3.62 (H-5), 3.55 (H-6), 5.62 (H-7), 6.57 (H-8), 6.65 (H-9), 6.45 (H-10), 7.26 (H-11), 5.92 (H-12), 6.27 (H-3′), 2.48 (H-4′), 1.16 ~ 1.25 (H-5′), 1.16-1.25 (H-6′), 1.16–1.25 (H-7′), 0.83 (H-8′), 1.77 (H-9′), 0.94 (H-10′), 2.52 (H-4″), 2.52 (H-5″). ^{13}C NMR (125 MHz, DMSO-d_6): δ 190.7 (C-1), 130.2 (C-2), 129.3 (C-3), 72.3 (C-4), 58.2 (C-5), 53.8 (C-6), 139.0 (C-7), 132.2 (C-8), 140.7 (C-9), 132.9 (C-10), 144.1 (C-11), 123.1 (C-12), 167.7 (C-13), 117.3 (C-1′), 130.7 (C-2′), 145.5 (C-3′), 34.3 (C-4′), 37.7 (C-5′), 30.8 (C-6′), 23.8 (C-7′), 14.4 (C-8′), 12.8 (C-9′), 20.4 (C-10′), 34.3 (C-4″), FABMS (+): m/z 511, $C_{28}H_{34}N_2O_7$; (Calc. 510.2366 for $C_{28}H_{34}N_2O_7$).

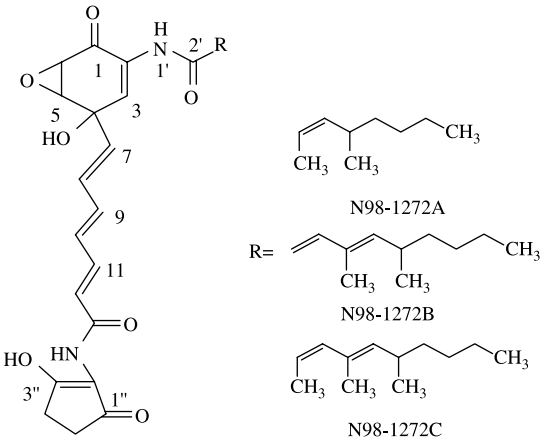

Figure 2. The structures of the N98-1272 A, B, C.

N98-1272 B (Manumycin C): Orange powder; UV (MeOH) λmax: 325.5 nm; ^{1}H NMR (500 MHz, DMSO-d_6): δ 7.15 (H-3), 3.69 (H-5), 3.50 (H-6), 6.48 ~ 6.58 (H-7), 6.48 ~ 6.58 (H-8), 6.48 ~ 6.58 (H-9), 6.76 (H-10), 7.23 (H-11), 6.42 (H-12), 6.01 (H-2′), 7.09 (H-3′), 5.70 (H-5′), 2.50 (H-6′), 1.20 ~ 1.40 (H-7′), 1.20 ~ 1.40 (H-8′), 1.20 ~ 1.40 (H-9′), 0.90 (H-10′), 1.01 (H-12′), 0.94 (H-13′), 2.58 (H-4″), 2.58(H-5″). ^{13}C NMR (125 MHz, DMSO-d_6): δ 189.4 (C-1), 128.6 (C-2), 128.1 (C-3), 70.6 (C-4), 56.5 (C-5), 52.4 (C-6), 139.3 (C-7), 131.2 (C-8), 139.6 (C-9), 131.2 (C-10), 142.1 (C-11), 122.4 (C-12), 165.2 (C-13), 165.9 (C-1′), 119.5 (C-2′), 146.8 (C-3′), 129.7 (C-4′), 32.5 (C-6′), 36.3 (C-7′), 29.1 (C-8′), 22.2 (C-9′), 13.9 (C-10′), 12.3 (C-11′), 20.4 (C-12′), 119.5 (C-2″), 22.2 (C-5″); FABMS (+): m/z 537, $C_{30}H_{36}N_2O_7$; (Calc. 536.2523 for $C_{30}H_{36}N_2O_7$).

N98-1272 C (Manumycin A): Orange powder; UV (MeOH) λmax: 286.3 nm, 324.3 nm; IR (KBr) νmax: 3380, 3240, 2900, 1680, 1600, 1500 cm^{-1}; ^{1}H NMR (500 MHz, DMSO-d_6): δ 7.29 (H-3), 3.63 (H-5), 3.57 (H-6), 5.89 (H-7), 6.67 (H-8), 6.65(H-9), 6.56 (H-10), 6.45 (H-11), 6.26 (H-12), 6.72 (H-3′), 5.29 (H-5′), 2.45 ~ 2.48 (H-6′), 1.20 ~ 1.35 (H-8′), 1.20 ~ 1.35 (H-9′), 0.85 (H-10′), 1.97 (H-11′), 1.78 (H-12′), 0.94 (H-13′). ^{13}C NMR (125 MHz, DMSO-d_6): δ 190.7 (C-1), 139.8 (C-2), 129.4 (C-3), 72.3 (C-4), 58.3 (C-5), 53.9 (C-6), 139.0 (C-7), 132.2 (C-8), 140.0 (C-9), 132.8 (C-10), 144.1 (C-11), 123.1 (C-12), 167.7 (C-13), 171.0 (C-1′), 130.2 (C-2′), 140.2 (C-3′), 131.6 (C-4′), 143.1 (C-5′), 34.3 (C-6′), 38.3 (C-7′), 29.8 (C-8′), 21.2 (C-9′), 14.9 (C-10′), 14.3 (C-11′), 16.7 (C-12′), 21.2 (C-13′), 116.3 (C-2″), 171.0 (C-3″), 31.1(C-4″), 24.0 (C-5″), FABMS (+): m/z 551, $C_{31}H_{38}N_2O_7$; (Calc. 550.2679 for $C_{31}H_{38}N_2O_7$).

Inhibition of acetylcholinesterase

The inhibitory effects of N98-1272 A, B, and C on AChE and BuChE are shown in Figures 4 and 5. All the three compounds were observed to have a similar inhibitory activity on AChE in a dose-dependent manner and the IC_{50} values of N98-1272 A, B and C were 15.0, 11.5 and 12.5 μM, respectively. However, the three compounds did not show any inhibitory effect on BuChE even at 100 μM. In our assay system, Tacrine, a positive control, inhibits both BuChE (IC_{50}, 0.18 μM) and AChE (IC_{50}, 9.2 μM). So compared with Tacrine, N98-1272 A, B, and C exhibit much better selectivity towards AChE.

Structure-activity relationship studies

To understand the structural constituents necessary for inhibition of AChE, the cyclohexenone epoxide moiety of N98-1272 C was removed by reduction and the inhibitory activity of this reduced N98-1272 C derivate was assayed. Strikingly, the deoxy-N98-1272 C (see Figure 3) had no inhibitory effect on AChE even at 100 μM (Figure 4). This result indicates that the cyclohexenone epoxide moiety is critical for the inhibitory effect of N98-1272 C on AChE. Considering the similar activities shown among the three isolated compounds, we believe that the cyclohexenone epoxide moieties of N98-1272 A, B and C are essential for their inhibition of AChE.

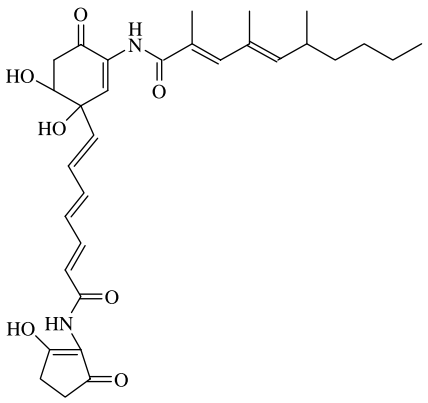

Figure 3. The structure of deoxy N98-1272C.

Kinetic studies

To investigate the mechanism of inhibition of AChE by N98-1272 C, kinetic analysis was carried out. Panel A of Figure 6 shows that the inhibition of AChE is dose-dependent and the inhibition appears to be reversible. The Hanes plot (Figure 6, panel B) at various concentrations of ATCh and N98-1272 C indicates that the presence of N98-1272 C does not change the Km value of AChE, but the V_{max} is apparently decreased, suggesting that N98-1272 C is a noncompetitive inhibitor. Therefore, N98-1272 C is likely to act as a reversible noncompetitive inhibitor

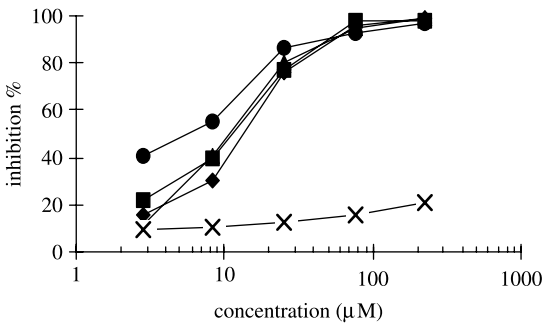

Figure 4. Inhibitory activity of tacrine (●), N98-1272A (◆), B (▲), C (■), and deoxy- N98-1272 C (×) to AChE.

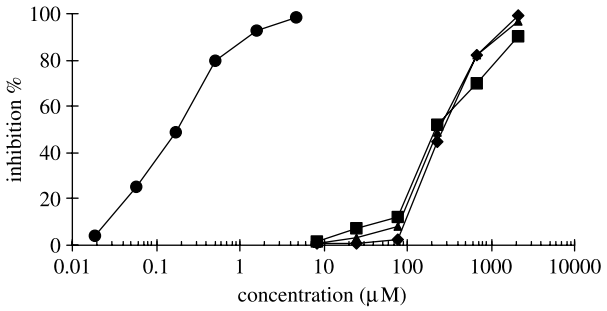

Figure 5. Inhibitory activity of tacrine (●), N98-1272 A (◆), B (▲), C (■) to BuChE.

of AChE. Analysis of the apparent V_{max} versus inhibitor concentration gave a *Ki* value of 7.2 μM (data not shown).

Discussion

N98-1272 A, B and C, the members of a large manumycin family isolated from actinomycete metabolites, were originally discovered as antibacterial antibiotics produced by *Streptomyces parvulus* strain Tu 64 and named Manumycins [7,8]. Manumycins and related compounds exhibit antibacterial, antifungal, and cytotoxic activities. Moreover they exhibit inhibitory effects on interleukin-1 converting enzyme and Ras farnesyltransferase [9–15]. We show here that Manumycins and Tacrine exhibit comparable inhibitory effects on AChE. However, Manumycins show much less inhibiton of BuChE than Tacrine, indicative of the better specificity of Manumycins toward AChE. Tacrine[16], the first approved drug for Alzheimer's disease, is able to significantly improve the cognitive function in Alzheimer's patients, but also causes hepatotoxic side effects due to inhibition of butyrylcholinesterase (BuChE) [17,18]. For this reason the search for selective inhibitors of AChE has attracted a lot of attention in recent years. The selectivity of many AChE inhibitors, including Tacrine bisfunctional analogues [19], huperzine A [20], arisugacins[21] and terreulactones [22] have been studied.

Kinetic studies indicated that N98-1272 C acts as a reversible noncompetitive inhibitor of AChE. A structure-activity relationship investigation revealed that the cyclohexenone epoxide moiety of N98-1272 C is critical for inhibition of AChE. Epoxide ring opening of N98-1272 C results in a significant decrease of its inhibitory activity against AChE. Strikingly, deoxy-N98-1272 C exhibits no inhibitory effect on AChE even at 100 μM. In order to gain insight into the structural basis by which N98-1272C (Manumycin A) exerts its inhibitory activity on AChE, we analyzed the active site of the AChE, the complex of AChE and Tacrine and performed molecular docking studies on Manumycin A into the AChE active site.

A number of studies have focused on the structural basis of the catalytic efficiency of AChE [23,24,25,26]. X-ray crystallography of *Torpedo californa* AChE (TcAChE) reveals that the active site of AChE lies at the bottom of a deep (20 Å) and narrow gorge, named the "active site gorge" or "aromatic gorge". A catalytic triad of Ser200-His440-Glu327 is responsible for hydrolyzing the ester bond in ACh. At the "anionic" subsite of the active site, adjacent to the catalytic triad, the indole side chain of the conserved residue Trp84 makes a cation-π interaction with the quaternary amino group of ACh. A second aromatic residue, Phe330, is also involved in recognition of quaternary ligands and ACh. The conserved residue Trp279 is the major component of a second binding site, named the peripheral "anionic" site (PAS), ~14 Å from the active site, near the top of the gorge. The crystal structure of the complex of TcAChE with Tacrine shows that Tacrine is stacked against Trp-84, sandwiched between the rings of Phe-330 and

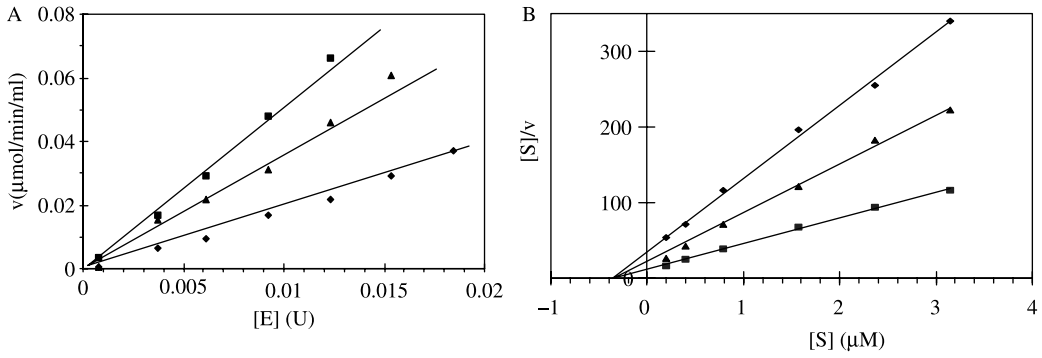

Figure 6. Kinetics plots of N98-1272 C to AChE. [A] A plot of v (μmol/min/mL) versus enzyme concentration [E] at different N98-1272 C concentration of 0 μM (■), 10 μM (▲), 20 μM (◆). [B] A Hanes plot of [S]/v versus [S] at N98-1272C of 0 M (■), 10 μM (▲), 20 μM (◆). Each point represents the average of 3 wells.

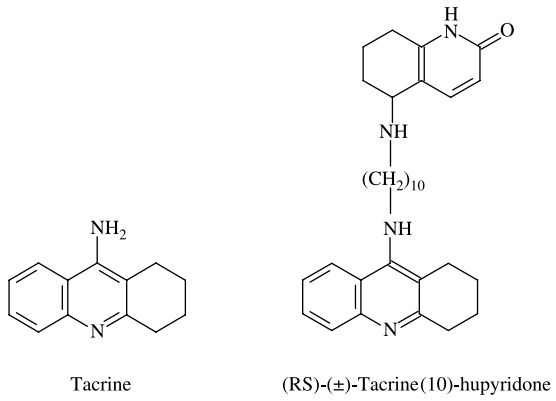

Figure 7. Reference AChE inhibitors.

Trp-84. The ring nitrogen of Tacrine forms a hydrogen-bond with the main-chain carbonyl oxygen of His-440, and the amino nitrogen also forms a hydrogen bond with a water molecule (Figure 8A). This series of non-covalent bond interactions with the key amino acids of the active anionic site allows Tacrine to block the hydrolysis of ACh catalyzed by AChE.

We applied a computational docking method with SYBYL software (Tropos Inc.) to dock the Manumycin A N98-1272 C into the crystal structure TcAChE complex with (RS)-(±)-Tacrine(10)-hupyridone (Figure 7), and found that part of Manumycin A might insert into the gorge of TcAChE. The 2-amino-3-hydroxycyclopent-2-enone moiety of Manumycin A may stack against Trp-84, sandwiched between the ring of Phe-330 and Trp-84 like Tacrine, but this π−π interaction is weaker than that of Tacrine with Trp-84 and Phe330. The π electron system of Tacrine is larger, and there is a H-bond interaction between the ring amino hydrogen of Tacrine and the carbonyl oxygen of H440. The all-trans triene mC7N chain moiety of Manumycin A lies along the aromatic gorge and the epoxide cyclohexenone moiety lies at the peripheral anionic site and interaction occurs with some of the amino acids of the aromatic gorge of AChE with the cyclohexenone epoxide structure (Figure 8B). Thus, the interaction of Manumycin A with AChE is mainly in the peripheral "anionic" site (the upper area of the aromatic gorge). When the epoxide ring of Manumycin A is open and reduced, as in the mono-hydroxyl-cyclohexenone structure, the deoxy-Manumycin A loses some H-bond interactions with some upper amino acids of the aromatic gorge of AChE, and the deoxy-Manumycin A molecule cannot tether near the active site of AChE.

Regarding the selective inhibition of AChE over BuChE by Manumycin A, we found that Manumycin A could not dock into the active site of BuChE. The most dramatic difference between BuChE and AChE is confined to the residues at the gorge, where BuChE has more aliphatic hydrophobic amino-acid residues but AChE contains more aromatic ones. We believe that the Manumycin A molecule is prone to interact with the aromatic groups instead of the hydrophobic groups.

Some recent studies have shown that Manumycin A is a neutral sphingomyelinase (nSMase) inhibitor [28] that prevents the generation of age-associated amyloid β-peptide by inhibiting the hydrolysis of sphingomyelin into the second messenger ceramide and blocks the activation of ceramide in the $P75^{NTR}$-ceramide signaling pathway. Thus, Manumycin A might be a good lead compound for the treatment of Alzheimer's disease.

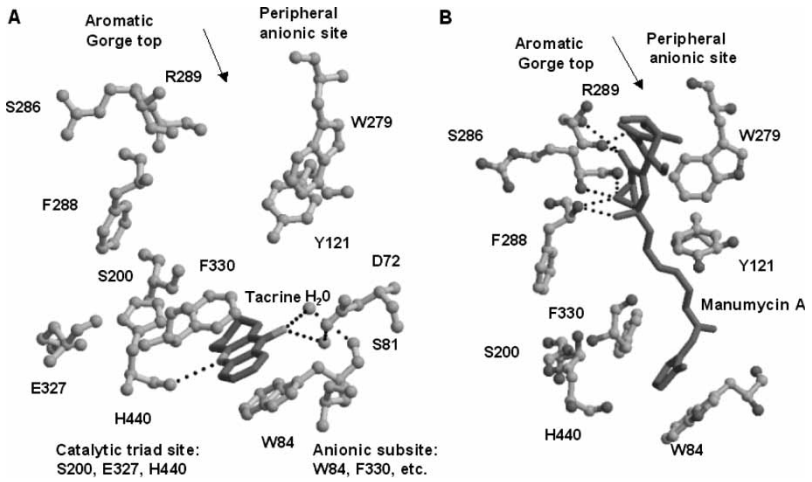

Figure 8. A. Overlay of the trigonal crystal structure of tacrine (black) and TcAChE (gray) complex: showing the catalytic anionic site, aromatic gorge, and peripheral anionic site [26]; B. Overlay of docking figure of the Manumycin A (black) into trigonal TcAChE (gray), showing the non-covalent binding between Manumycin A with the amino acids at the aromatic gorge of TcAChE.

Acknowledgements

This work was supported by the Chinese Ministry of Science and Technology in Mega-projects of Science Research for the 10th Five-Year Plan (Grant No. 2002AA2Z343D). We wish to express our thanks to Professor Yanchang Wang and Professor Randy Rill (Department of Biomedical Sciences, College of Medicine, Florida State University, U.S.A), Dr. Shaun K. Olsen and Dr. Yong Xie (Riken, Yokohama Institute, Japan) for their help in English revision and valuable suggestions.

References

[1] Warner J, Butler R, Arya P. Dementia. Clin Evid 2004;12:1361–1390.

[2] Whitehouse PJ, Struble RG, Hedreen JC, Clark AW, White CL, Parhad IM, Price DL. Neuroanatomical evidence for a cholinergic deficit in Alzheimer's disease. Psychopharmacol Bull 1983;19:437–440.

[3] Roberts F, Lazareno S. Cholinergic treatments for Alzheimer's disease. Biochem Soc Trans 1989;17:76–79.

[4] William ER. Current pharmacologic options for patients with Alzheimer's disease. Ann Gen Hosp Psych 2003;2:1–12.

[5] Jiang Y, Li WJ, Cui XL, Zhang H, Xu LH, Jiang CL. Polyphasic classification of *Streptomyces bannaenesis* sp.nov. J Yunnan Uni 2004;26:179–182.

[6] Ellman GL, Courtney KD, Andres V, Featherstone RM. *In vitro* effects of various cholinesterase inhibitors on acetyl- and butyrylcholinesterase of healthy volunteers. Biochem Pharmacol 1961;7:88–95.

[7] Zeeck A, Schroder K, Frobel K, Grote R, Thuerucke R. The Structure of Manumycin. I. Characterization. J Antibiot 1987;40:1530–1540.

[8] Zeeck A, Frobel K, Heusel C, Schroder K, Thiericke R. The Structure of Manumycin. II. Derivatives. J Antibiot 1987;40:1541–1548.

[9] Shu YZ, Huang S, Wang RR, Lam KS, Klohr SE, Volk KJ, Pirnik DM, Wells JS, Fernandes PB, Patel PS, Manumycins E, F and G, new members of Manumycin class antibiotics, from *Streptomyces* sp. J Antibiot 1994;47:324–333.

[10] Nayashi K, Nakagawa M, Fujita T, Tanimori S, Nakayama M. Nisamycin, a new Manumycin group antibiotic from *Streptomyces* sp. K106. J Antibiot 1993;46:1904–1907.

[11] Franco CM, Maurya R, Vijayakumar EK, Chatterjee S, Blumbach J, Ganguli BN. Alisamycin, a new antibiotic of the Manumycin group. I. Taxonomy, production, isolation and biological activity. J Antibiot 1991;44:1289–1293.

[12] Kohno J, Nishio M, Kawano K, Nakanishi N, Suzuki S, Uchida T, Komatsubara S. TMC-1 A B C and D new antibiotics of the Manumycin group produced by *Streptomyces* sp. Taxonomy, production, isolation, physico-chemical properties, structure elucidation and biological properties. J Antibiot 1996;49:1212–1220.

[13] Hara M, Akasaka K, Akinaga S, Okabe M, Nakano H, Gomez R, Wood D, Uh M, Tamanoi F. Identifiction of Ras farnesyltransferase inhibitors by microbioal screening. Proc Natl Acad Sci USA 1993;90:2281–2285.

[14] Tanaka T, Tsukuda E, Uosaki Y, Matsuda Y. EI-1511-3-5 and EI-1625-2, Novel Interleukin-1β converting enzyme inhibitions produced by *Streptomyces* sp. E-1511 and E-1625, III. Biochemical properties of E-1511 and E-1625. J Antibiot 1996;49:1085–1090.

[15] Yeung SC, Xu G, Pan J, Christgen M, Bamiagis A. Manumycin enhances the cytotoxic effect of paclitaxel on anaplastic thyroid carcinoma cells. Cancer Res 2000;60:650–656.

[16] Ibach B, Haen E. Acetylcholinesterase inhibition in Alzheimer's disease. Curr Pharm Des. 2004;10:231–251.

[17] Pacheco G, Palacios-esquivel R, Moss DE. Cholinesterase inhibitors proposed for treating dementia in Alzheimer's disease: Selectivity toward human brain acetylcholinesterase compared with butyrylcholinesterase. J Pharmacol Exp Ther 1995;274:767–770.

[18] Thomsen T, Zendeh B, Fischer JP, Kewitz H. *In vitro* effects of various cholinesterase inhibitors on acetyl-and butyrylcholinesterase of healthy volunteers. Biochem Pharmacol 1991;41:139–141.

[19] Pang YP, Quiram P, Jelacic T, Hong F, Brimijoin S. Highly potent, selective, and low cost bis-tetrahydroaminacrine inhibitors of acetylcholinesterase. Steps toward novel drugs for treating Alzheimer's disease. J Biol Chem 1996;271: 23646–23649.

[20] Raves ML, Harel M, Pang YP, Silman I, Kozikowski AP, Sussman JL. Structure of acetylcholinesterase complexed with the nootropic alkaloid, (-)-huperzine A. Nat Struct Biol 1997;4:57–63.

[21] Kuno F, Otoguro K, Shiomi K, Iwai Y, Omura S. Arisugacins A and B, novel and seletive acetylcholinesterase inhibitors from *Penicillium* sp. FO-4259, I. Screening, taxonomy, fermentation, isolation and biological activity. J Antibiot 1996;49:742–747.

[22] Cho KM, Kim WG, Lee CK, Yoo ID. Terreulactones A, B, C, and D: Novel acetylcholinesterase inhibitors produced by *Aspergillus terreus*. I. Taxonomy, fermentation, isolation and biological activities. J Antibiot 2003;56:344–350.

[23] Harel M, Schalk I, Ehret-Sabatier L, Bouet F, Goelder M, et al. Quaternary ligand binding to aromatic residues in the active-site gorge of acetylcholinesterase. Proc Natl Acad Sci USA 1993;90:9031–9035.

[24] Johnson JL, Cusack B, Hughes TF, McCullough EH, Fauq A, Romanovskis P, Spatola AF, Rosenberry TL. Inhibitors tethered near the acetylcholinesterase acitive site serve as molecular rulers of the peripheral and acylation sites. J Biol Chem 2003;278:38948–38955.

[25] Bar-On P, Millard CB, Harel M, Dvir H, Enz A, Sussman JL, Silman I. Kinetic and structural studies on the interaction of cholinesterases with the anti-Alzheimer drug rivastigmine. Biochemistry 2002;41:3555–3564.

[26] Haviv H, Wong DM, Greenblatt HM, Carlier PR, Pang YP, Silman I, Sussman JL. Crystal packing mediates enantioselective ligand recognition at the peripheral site of acetylcholinesterase. J Am Chem Soc 2005;127:11029–11036.

[27] Nicolet Y, Lockridge O, Masson P, Fontecilla-Camps JC, Nachon F. Crystal structure of human butyrylcholinesterase and of its complexes with substrate and products. J Biol Chem 2003;278:41141–41147.

[28] Costantini C, Weindruch R, Della Valle R, Puglielli L. A TrKA-to-p75^{NTR} molecular switch activates amyloid β-peptide generation during aging. Biochem J 2005;391:59–67.